

# **17NRM03 EUCoM**

*Evaluating Uncertainty in Coordinate Measurement*

Report describing the procedure for a posteriori type A evaluation of measurement uncertainty

**DELIVERABLE D1**

Lead partner: AIST

*Osamu Sato and Alessandro Balsamo*

Deliverable Due Date: March 2021

Actual Submission Date: 2021-12-24

## Table of Contents

1. Abstract .....	3
2. Introduction .....	4
3. Procedure.....	6
3.1 Measurements .....	6
3.1.1 Multiple measurements on the workpiece .....	6
3.1.2 Measurements of standards of length .....	7
3.1.3 Measurements of a test sphere .....	8
3.2 Calculation of the measurement value.....	10
3.2.1 Calculation of the uncorrected measurement value $y$ .....	10
3.2.2 Calculation of the average scale error $E_S$ .....	10
3.2.3 Calculation of the probe size error $E_D$ .....	10
3.2.4 Calculation of the probe location error $E_{PrbLoc}$ .....	10
3.2.5 Calculation of the measurement value $y_{corr}$ corrected error for scale and/or probe size errors .....	11
3.3 Evaluation of the measurement uncertainty.....	11
3.3.1 Evaluation of $u_{rep}$ and $u_{geo}$ .....	12
3.3.2 Evaluation of $u_S$ .....	14
3.3.3 Evaluation of $u_D$ .....	18
3.3.4 Evaluation of $u_{PrbLoc}$ .....	22
3.3.5 Evaluation of $u_{geo \times dist}$ .....	22
3.3.6 Evaluation of $u_{temp}$ .....	26
3.4 Special cases .....	26
3.4.1 Poor available information .....	26
3.4.2 Extension to scanning.....	28
3.4.3 Prismatic tolerance zones.....	28
3.4.4 Constrained features .....	30
3.4.5 Profile tolerances .....	30
4. Conclusions.....	31
5. References.....	32

## 1. Abstract

This report is concerned with an *a posteriori* (type A) uncertainty evaluation method developed in the work package 1 (WP1) of the EUCoM project. The WP1 resulted in a procedure based on multiple measurements taken by coordinate measuring machines (CMM) for evaluating the task-specific measurement uncertainty *a posteriori*. Through it, the measured values and the measurement uncertainties of products' geometrical features are calculated by a simple spreadsheet application based on the analysis of variance (ANOVA). This spreadsheet can easily run on the computers that are ordinarily available at the CMM and at the manufacturing floor.

## 2. Introduction

This document describes a method and related procedures for the evaluation of task-specific measurement uncertainty using coordinate measuring systems (CMSs [1]). The method applies to Cartesian coordinate measuring machines (CMMs) equipped with tactile probing systems. Nonetheless, its overall approach may be applicable to other types of CMSs as well (for instance, see [2] for an application to X-ray computer tomography).

A possible application of the method is for calibration of workpieces then used as *calibrated workpieces* in ISO 15530-3 [3]. Another possible application is the conformity verification of workpieces against their geometrical specifications in accordance with ISO 14253-1 [4].

The overall procedure consists of three steps:

1. multiple measurements of the workpiece;
2. measurements of length standards, and
3. measurements of a test sphere.

All measurements are carried out in the same portion of the CMM measuring volume.

The multiple measurements are performed by repetition with several workpiece orientations with identical distribution of probing points. The measurements of length standards—such as a gauge block—are executed with the standard in three directions perpendicular to one another, typically along the  $X$ ,  $Y$  and  $Z$  axes of the CMM; this is intended to capture the CMM scale errors, including thermal effects. The measurements of a test sphere with all probe styli used for the previous steps is intended to investigate the probe errors.

In principle, the feature of the workpiece shall be evaluated for its integral real surface. Practically, a finite number of points are sampled and an ideal surface is associated (integral feature associated to the extracted measured points sampled on the real surface). A common problem in the ISO GPS (Geometrical Product Specifications) is how to validate a real surface based on a limited number of sampled points.

In the case of a tactile CMMs, the number of the measured points is usually not very large. This implies that high-frequency components of the surface are not captured.

Figure 1 illustrates the form measurement with the extracted measured points, based on the concept in ISO 4287 [5]. In the case of surface texture parameter verification, the scope of the measurement is focused on the high-frequency components of the primary profile obtained on the physical surface. To put it the other way around, relatively low-frequency components of the primary profile are of interest in the case of form feature verification.

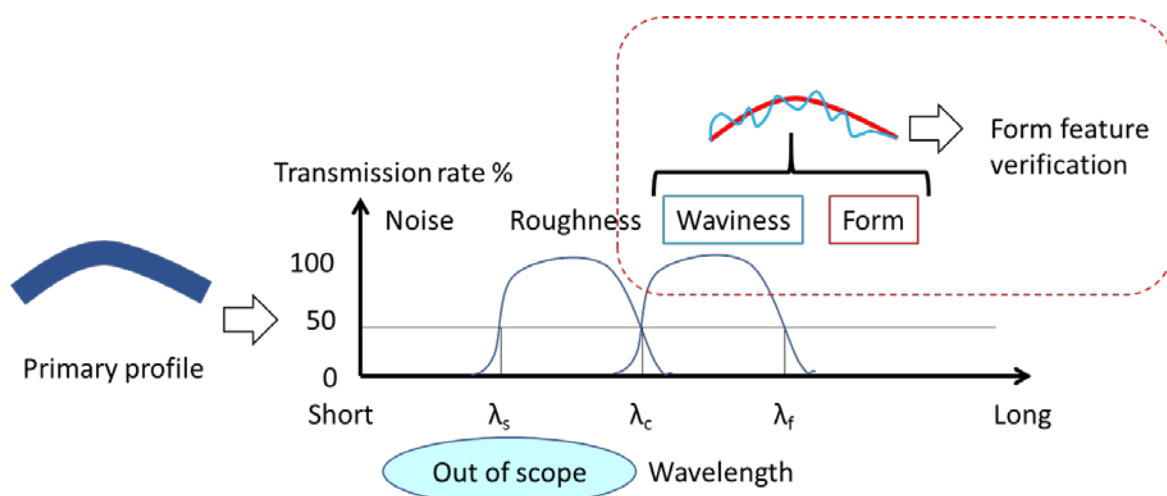


Figure 1 concept of form measurement with the extracted measured points

With the method reported in this document, a limited number of measured points is used to verify conformity of features. BS 7172 [6] gives guidance and recommendations on the minimum number of measured points for the assessment of geometrical features: position, size and form errors. However, the recommended number of points is small: at most 15. In contrast, ISO 12181-2 [7] provides a larger, but still manageable number of measurement points to evaluate relatively low-frequency components of feature, e.g., 105 points for 1<sup>st</sup> to 15<sup>th</sup> components of roundness. In this document, it is assumed that the features under verification are associated with at most a few hundred measured points.

The concept of the method in this document is similar to that in the ISO/DTS 15530-2 (2007) [8] by Dr. Eugen Trapet, which is listed as ISO/TC 213 N 940 in the ISO/TC 213 internal document server. This was the outcome of an ISO/TC 213/WG 10 project, which was brought to the stage of DTS (*Draft Technical Specification*) and then abandoned for lack of resources. In turn, that project had its roots in an earlier European project [9]. The underlying principle of the procedure in this document is found in Clause 6 of the DTS [8].

## 3. Procedure

### 3.1 Measurements

#### 3.1.1 Multiple measurements on the workpiece

The workpiece is measured in four orientations as a default [10] [11]. Measurements in more orientations may be performed to better randomize systematic effect. Figure 2 shows an example of the measurement setup of a workpiece on the CMM. An orientation is referred to as "home position". The others are example orientations to randomize the systematic effects of the CMM. Four orientations are recommended, obtained by rotating the artefact at *home position* 90° in turn about the first, the second and the third axis of the CMM.

The measurements are carried out with an identical distribution of measured points<sup>1</sup> (same sampling pattern), i.e., the number and nominal locations of the measured points for extraction (see, ISO 14406 [12]) is the same for all positions. In the case that the method applies for calibrating the workpiece, the actual distribution of the measured points shall be recorded.

The number of repetitions for each orientation is three<sup>2</sup> by default. When a CMM is known to have poor repeatability<sup>3</sup>, the number of repetitions may be increased, to the discretion of the CMM user.

The results of all these measurements are the values  ${}^jy_i$  (see Table 1), where  $j = 1 \dots n_2$  indicates the orientation and  $i = 1 \dots n_1$  the repeat in a same orientation.

---

<sup>1</sup> The distributions of measurement points in the DTS [8] are randomized for the different positions. This aims at eliminating the unknown CMM systematic errors by averaging. However, it is hard to provide randomly varied distributions of measurement points when CMMs are operated under numerical control. In this document, the sampling pattern is kept identical for all position for sake of practicality.

<sup>2</sup> In the DTS, the default number of repetitions for the artefact measurement is at least five. In contrast, this document proposes three. A reason is for consistency with the number of repetitions for length and diameter standards (3). Another reason is that the variations of the measurement results by identical distributions of measurement points using well-maintained CMMs are not so large.

<sup>3</sup> For example, if the CMM exhibited a large  $R_0$  value, or is specified with a large  $R_{0,MPE}$  value (if no actual tests were performed), according to ISO 10360-2 [13].

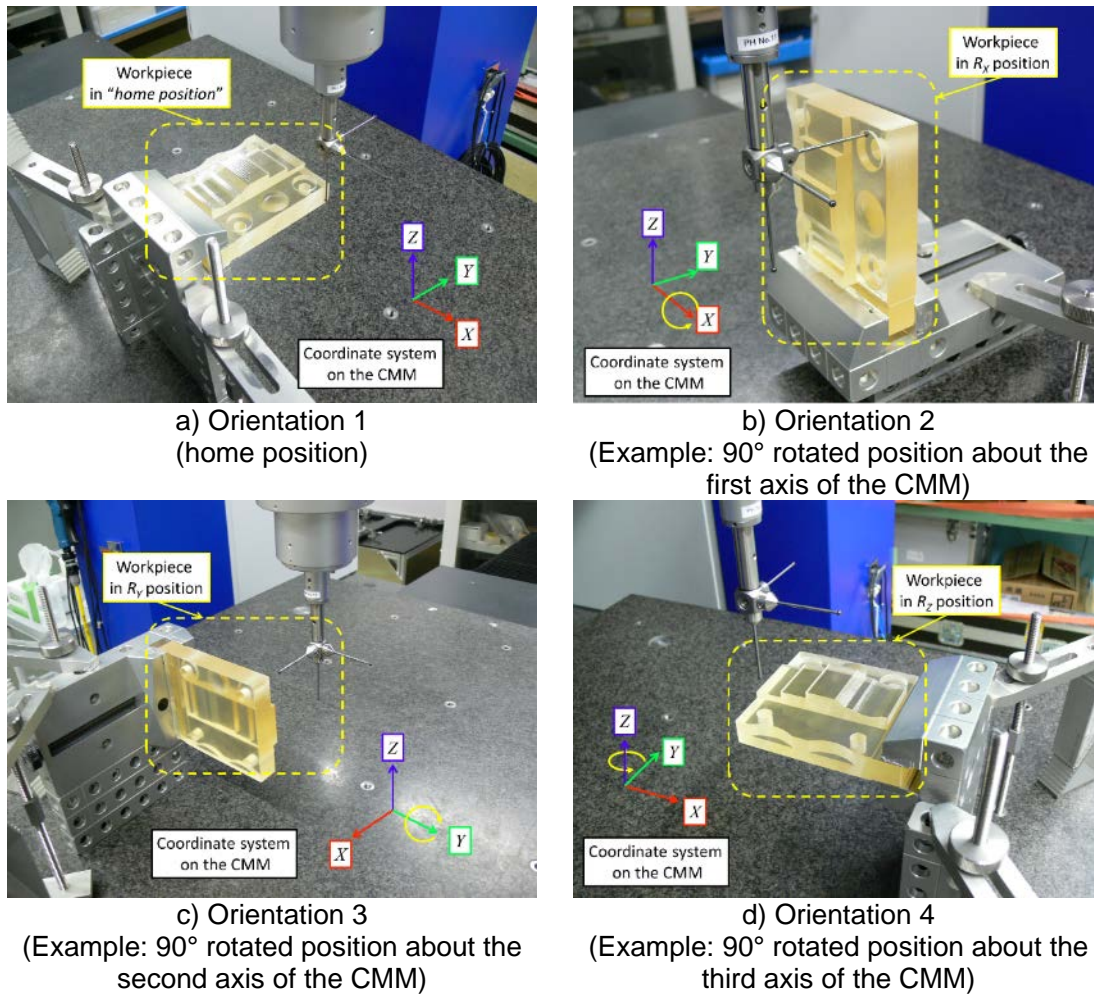


Figure 2 example of measurement setup of the workpiece in four orientations

Table 1 Summary of measurement results of the workpiece

	Orientation 1 (home position)	Orientation 2	Orientation 3	Orientation 4
Repeat 1	$1^1y$	$1^2y$	$1^3y$	$1^4y$
Repeat 2	$2^1y$	$2^2y$	$2^3y$	$2^4y$
Repeat 3	$3^1y$	$3^2y$	$3^3y$	$3^4y$

### 3.1.2 Measurements of standards of length

Material standards of length are measured in the same portion of the CMM volume where the workpiece is measured. The measurements of these standards are performed in at least three orientations approximately orthogonal to each other, typically aligned to the CMM axes. Figure 3 shows an example setup.

The results of the measurements of the length standards are used for two purposes: the compensation of the scale error of the CMM in the region of interest and the evaluation of the uncertainty derived from that scale error compensation. Ideally, the scale error values should be detected without the influence of probing errors. Therefore, it is recommended to carry out unidirectional measurements of the length standards (see Annex B of ISO 10360-2 [13] or  $E_{Vol}$  currently discussed in ISO/TC 213/WG 10 [14]).

In each orientation, the length standards are measured three times. When the CMM repeatability is known to be poor<sup>4</sup>, the number of repetitions shall be larger (e.g. 5).

Results are the values  ${}^{ij}L_{\text{measstd}}$  (see Table 2), where  $j = 1 \dots n_4$  indicates the orientation and  $i = 1 \dots n_3$  the repeat in a same orientation.

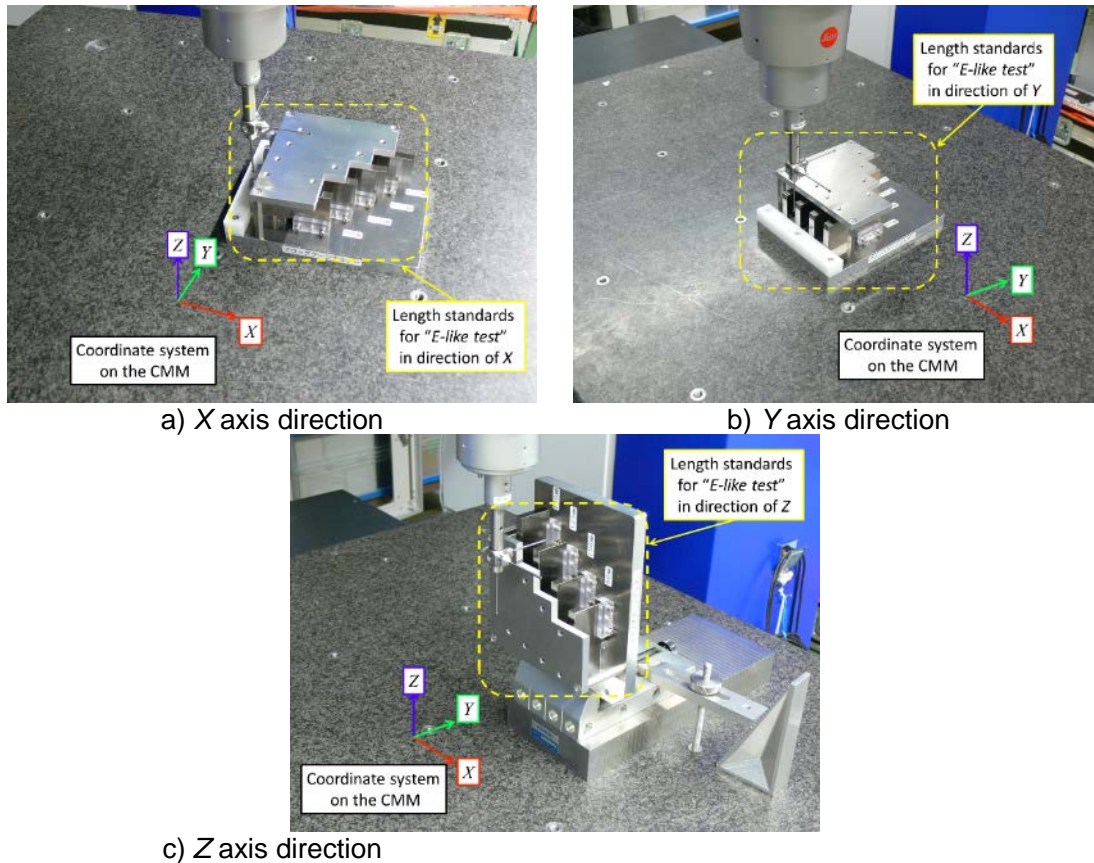


Figure 3 measurement setup of the length standard in three mutually-orthogonal directions.

Table 2 Summary of measurement results of the length standards

	Orientation 1 (X axis direction)	Orientation 2 (Y axis direction)	Orientation 3 (Z axis direction)
Repeat 1	${}^{11}L_{\text{measstd}}$	${}^{12}L_{\text{measstd}}$	${}^{13}L_{\text{measstd}}$
Repeat 2	${}^{21}L_{\text{measstd}}$	${}^{22}L_{\text{measstd}}$	${}^{23}L_{\text{measstd}}$
Repeat 3	${}^{31}L_{\text{measstd}}$	${}^{32}L_{\text{measstd}}$	${}^{33}L_{\text{measstd}}$

### 3.1.3 Measurements of a test sphere

The material standards of form are measured in the same portion of the CMM volume where the workpiece is measured. The material standard of form shall be different from the reference

<sup>4</sup> See previous footnote 3.



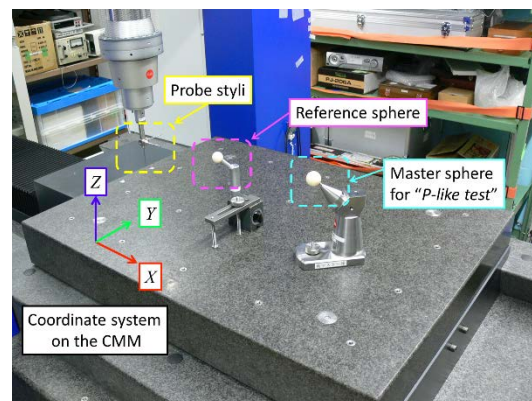
sphere used for the probe qualification [15]. It is recommended to use a test sphere as the material standard of form<sup>5</sup>. Figure 4 shows an example setup.

The measurement results are used for two purposes: the compensation of the CMM probing size error and the evaluation of the uncertainty incurred in probing<sup>6</sup>.

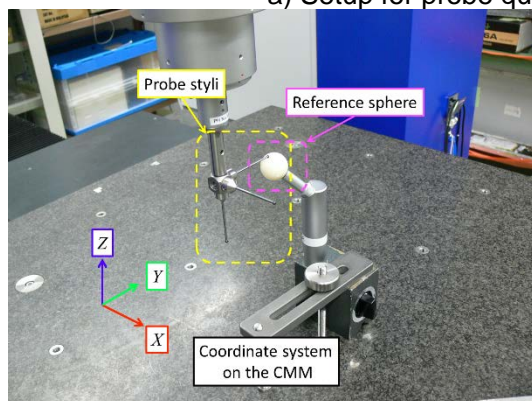
The test sphere is measured at least once with each probe stylus used for measuring the workpiece and the length standards, with a minimum of three measurements. The distribution of points (sampling pattern) is identical for all. By default, it is with 25 points evenly distributed over the accessible surface of the test sphere, as described in ISO 10360-5 [15].

With each stylus, the test sphere is measured three times. When the CMM repeatability is known to be poor<sup>7</sup>, the number of repetitions shall be larger (e.g. 5).

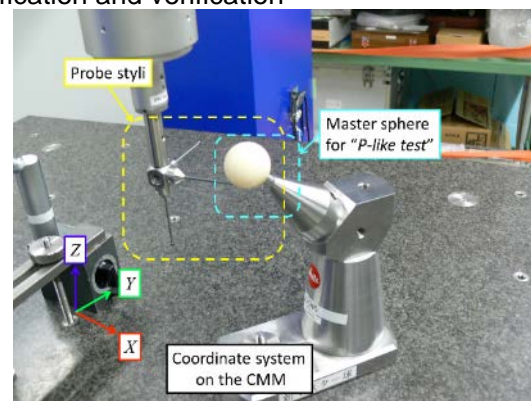
The least squares diameter and centre coordinates of the test sphere are derived for each measurement. Results are the values  ${}^{ij}D_{\text{measstd}}$  (see Table 3), where  $j = 1 \dots n_6$  indicates the probe stylus and  $i = 1 \dots n_5$  the repeat with a same probe stylus. Further, the diameters of the minimum circumscribed spheres enclosing the  $n_6$  sphere centres [15] at the same repeat (the  $n_6$  centres at the  $i = 1$  repeat, at the  $i = 2$  repeat, and so on) are derived. They are indicated as  ${}^iD_{\text{MCS}}$  in Table 3.



a) Setup for probe qualification and verification



b) Probe qualification



c) Probe verification

Figure 4 Measurement setup for probe qualification and verification.

<sup>5</sup> In the ISO/DTS 15530-2 [8], both internal and external diameter standards were used. In contrast, an external diameter standard only (a test sphere) is recommended here.

<sup>6</sup> This includes not only probing size and location errors but probing form errors as well.

<sup>7</sup> See previous footnote 3.

Table 3 Summary of measurement results of the sphere used for probe verification

	Probe 1	Probe 2	Probe 3	Centre
Cycle 1	$^{11}D_{\text{measstd}}$	$^{12}D_{\text{measstd}}$	$^{13}D_{\text{measstd}}$	$^1D_{\text{MCS}}$
Cycle 2	$^{21}D_{\text{measstd}}$	$^{22}D_{\text{measstd}}$	$^{23}D_{\text{measstd}}$	$^2D_{\text{MCS}}$
Cycle 3	$^{31}D_{\text{measstd}}$	$^{32}D_{\text{measstd}}$	$^{33}D_{\text{measstd}}$	$^3D_{\text{MCS}}$

### 3.2 Calculation of the measurement value

The method may apply with or without corrections of the length and probing errors, as detected through the measurements of the length standards and test sphere.

#### 3.2.1 Calculation of the uncorrected measurement value $y$

The average  $y$  of all measurements is called "uncorrected measurement value", which is calculated as

$$y = \frac{1}{n_1 \cdot n_2} \cdot \sum_{j=1}^{n_2} \sum_{i=1}^{n_1} ij y.$$

#### 3.2.2 Calculation of the average scale error $E_S$

The average scale error  $E_S$  in the region of interest is evaluated as

$$E_S = \frac{1}{n_3 \cdot n_4} \cdot \sum_{j=1}^{n_4} \sum_{i=1}^{n_3} (ij L_{\text{measstd}} - L_{\text{calstd}}),$$

where,  $L_{\text{calstd}}$  is the calibrated value of the length standard<sup>8</sup>.

#### 3.2.3 Calculation of the probe size error $E_D$

The probe size error  $E_D$  associated with the set of used probe styli is evaluated as

$$E_D = \frac{1}{n_5 \cdot n_6} \cdot \sum_{j=1}^{n_6} \sum_{i=1}^{n_5} (ij D_{\text{measstd}} - D_{\text{calstd}}),$$

where,  $D_{\text{calstd}}$  is the calibrated value of the test sphere diameter.

#### 3.2.4 Calculation of the probe location error $E_{\text{PrbLoc}}$

The probe location error  $E_{\text{PrbLoc}}$  associated with the set of used styli is evaluated as

$$E_{\text{PrbLoc}} = \frac{1}{n_5} \cdot \sum_{i=1}^{n_5} i D_{\text{MSC}}.$$

<sup>8</sup> This equation holds in the likely case that a single length standard is used, and then a single calibrated value exists. When more are used, the differences in the summation are taken to the relevant calibrated value. The double summation gets split in two: the external summation over the different length standards  $j$ , and the internal one over the repeats  $i$ .

### 3.2.5 Calculation of the measurement value $y_{\text{corr}}$ corrected error for scale and/or probe size errors

When the scale and/or probe size errors are corrected, the corrected value  $y_{\text{corr}}$  depends on the type of feature, as shown in Table 4.

Table 4 Values corrected for scale and probe size errors

Angle size	$y$
Angle distance	$y$
Radius (external)	$y - E_S - E_D/2$
Radius (internal)	$y - E_S + E_D/2$
Length size (external)	$y - E_S - E_D$
Length size (internal)	$y - E_S + E_D$
Length distance	$y - E_S$
Deviations from a CAD element Geometrical features related to datums Profile features on prismatic and "freeform" artefacts	$y - E_S$
Deviation from a least squares fitted element Geometrical features not related to datums	$y$

### 3.3 Evaluation of the measurement uncertainty

The measurement uncertainty of the measurand feature is derived as [11]

$$U = k \cdot \sqrt{|E_S|^2 + |E_D|^2 + |E_{\text{PrbLoc}}|^2 + \frac{u_{\text{rep}}^2}{n_1} + \frac{u_{\text{geo}}^2}{n_2} + u_{\text{geo} \times \text{dist}}^2 + u_S^2 + u_D^2 + u_{\text{PrbLoc}}^2 + u_{\text{temp}}^2}$$

where:

- $U$  combined expanded uncertainty,
- $k$  coverage factor,
- $E_S$  average scale error of the CMM in the region of interest,
- $E_D$  average probe size error,
- $E_{\text{PrbLoc}}$  average probe location error,
- $u_{\text{rep}}$  standard uncertainty due to repeatability,
- $u_{\text{geo}}$  standard uncertainty due to the CMM geometry errors,
- $u_{\text{geo} \times \text{dist}}$  standard uncertainty due to the interaction between the CMM geometry errors and the distribution of points over the measured surface,
- $u_S$  standard uncertainty due to the scale error,
- $u_D$  standard uncertainty due to the probe size error,
- $u_{\text{PrbLoc}}$  standard uncertainty due the probe location error, and

$u_{temp}$  standard uncertainty due to temperature-related effects.

$|E_S|$  and/or  $|E_D|$  are to be accounted only when the scale and/or probe size errors are not corrected for.  $|E_S| = |E_D| = 0$  when they are.

$|E_D|$  is to be accounted for only for measurements sensitive to the stylus tip radius (bidirectional probing).  $|E_D| = 0$  for measurements that are not (monodirectional probing).

$|E_{PrbLoc}|$  and  $u^2_{PrbLoc}$  are to be accounted only when multiple probe styli are used in a same orientation of the workpiece.  $|E_{PrbLoc}| = 0$  and  $u^2_{PrbLoc} = 0$  when a single probe stylus is used in a same orientation of the workpiece.

$u^2_{geo \times dist}$  is there only in the case of measurements of the deviation from CAD or associated (best-fitted) elements (form error of either a profile or a surface).

### 3.3.1 Evaluation of $u_{rep}$ and $u_{geo}$

$u_{rep}$  and  $u_{geo}$  are evaluated following an analysis of variance (ANOVA) approach. The repeats are considered as *groups* (subscript A) of observations affected by a random error (subscript e), and the *within* and *between* variances are evaluated. The sought  $u_{rep}$  and  $u_{geo}$  are then derived from such variances.

Table 5 summarises the ANOVA approach for evaluating  $u_{rep}$  and  $u_{geo}$ .

Table 5 Evaluation of  $u_{rep}$  and  $u_{geo}$  (ANOVA).

${}^j\bar{y} = \frac{1}{n_1} \sum_{i=1}^{n_1} {}^{ij}y$			
$\bar{y} = \frac{1}{n_1 n_2} \sum_{i=1}^{n_1} \sum_{j=1}^{n_2} {}^{ij}y$			
Sum of squares	Degrees of freedom (DOF)	Variance	Expectation of
$S_A = \sum_{i=1}^{n_1} \sum_{j=1}^{n_2} ({}^j\bar{y} - \bar{y})^2$	$f_A = n_2 - 1$	$V_A = \frac{S_A}{f_A}$	$u_{rep}^2 + n_1 u_{geo}^2$
$S_e = \sum_{i=1}^{n_1} \sum_{j=1}^{n_2} ({}^{ij}y - {}^j\bar{y})^2$	$f_e = (n_1 - 1)n_2$	$V_e = \frac{S_e}{f_e}$	$u_{rep}^2$
$S = \sum_{i=1}^{n_1} \sum_{j=1}^{n_2} ({}^{ij}y - \bar{y})^2$	$f = n_1 n_2 - 1$		
$u_{rep}^2 = V_e$			
$u_{geo}^2 = \frac{V_A - V_e}{n_1}$			

Example: angle between two planes.

The following example illustrates the uncertainty evaluation for the measurement of the angle size between two planes. Both planes are measured with a single stylus in each orientation (see Figure 5).

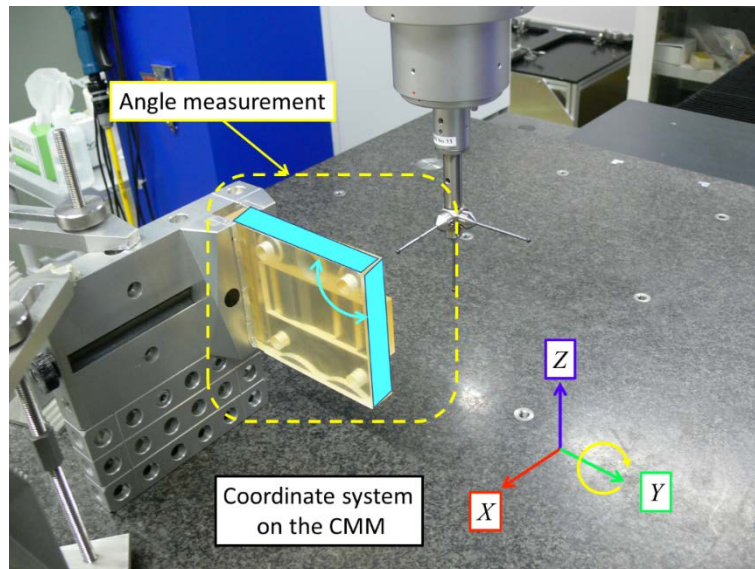


Figure 5 Measurement of the angle size between two planes (Orientation 3).

Example: angle between two planes.

	Orientation 1 (home position)	Orientation 2	Orientation 3	Orientation 4
Repeat 1/°	90.0033	90.0039	90.0033	89.9964
Repeat 2/°	90.0033	90.0040	90.0035	89.9963
Repeat 3/°	89.9967	90.0040	90.0036	89.9963
$\bar{y}^j/^\circ$	90.0011	90.0040	90.0035	89.9963
$\bar{y}/^\circ$	90.0012			

$S/(^{\circ 2})$	DOF	Variance/( $^{\circ 2}$ )	Expectation of
$S_A = \sum_{i=1}^{n_1} \sum_{j=1}^{n_2} (j\bar{y} - \bar{y})^2 = 0.000\ 110$	$f_A = n_2 - 1 = 3$	$V_A = \frac{S_A}{f_A} = 0.000\ 037$	$u_{\text{rep}}^2 + n_1 u_{\text{geo}}^2 = u_{\text{rep}}^2 + 3u_{\text{geo}}^2$
$S_e = \sum_{i=1}^{n_1} \sum_{j=1}^{n_2} (ijy - j\bar{y})^2 = 0.000\ 029$	$f_e = (n_1 - 1) \cdot n_2 = 8$	$V_e = \frac{S_e}{f_e} = 0.000\ 004$	$u_{\text{rep}}^2$
$S = \sum_{i=1}^{n_1} \sum_{j=1}^{n_2} (ijy - \bar{y})^2 = 0.000\ 139$	$f = n_1 \cdot n_2 - 1 = 11$		
$u_{\text{rep}}^2 = V_e = 0.000\ 004^{\circ 2}$			
$u_{\text{geo}}^2 = (V_A - V_e)/n_1 = 0.000\ 011^{\circ 2}$			
$U = k \cdot \sqrt{\frac{u_{\text{rep}}^2}{n_1} + \frac{u_{\text{geo}}^2}{n_2}} = 3 \sqrt{\frac{0.000\ 004}{3} + \frac{0.000\ 011}{4}} = 0.006^{\circ}$			

### 3.3.2 Evaluation of $u_s$

The uncertainty of the average scale error,  $u_s$ , is evaluated as

$$u_s^2 = \left(\frac{U_{\text{calstd,L}}}{2}\right)^2 + \frac{u_{\text{measstd,L,rep}}^2}{n_3} + \frac{u_{\text{measstd,L,geo}}^2}{n_4},$$

where,  $U_{\text{calstd,L}}$  is the expanded calibration uncertainty ( $k = 2$ ) of the length standard.  $u_{\text{measstd,L,rep}}$  and  $u_{\text{measstd,L,geo}}$ , are evaluated following an analysis of variance (ANOVA) approach. Table 6 summarises the ANOVA approach for evaluating  $u_{\text{measstd,L,rep}}$  and  $u_{\text{measstd,L,geo}}$  and the evaluation of  $u_s$ .

Table 6: Evaluation of  $u_{\text{measstd,L,rep}}$  and  $u_{\text{measstd,L,geo}}$  (ANOVA).

$j\overline{\overline{L}}_{\text{measstd}} = \frac{1}{n_1} \sum_{i=1}^{n_1} ijL_{\text{measstd}}$
$\overline{\overline{\overline{L}}}_{\text{measstd}} = \frac{1}{n_1 n_2} \sum_{i=1}^{n_1} \sum_{j=1}^{n_2} ijL_{\text{measstd}}$

Sum of squares	Degrees of freedom (DOF)	Variance	Expectation of
$S_A = \sum_{i=1}^{n_3} \sum_{j=1}^{n_4} \left( \overline{jL_{\text{measstd}}} - \overline{\overline{L_{\text{measstd}}}} \right)^2$	$f_{iA} = n_4 - 1$	$V_A = \frac{S_A}{f_A}$	$u_{\text{measstd,L,rep}}^2 + n_3 \cdot u_{\text{measstd,L,geo}}^2$
$S_e = \sum_{i=1}^{n_3} \sum_{j=1}^{n_4} \left( {}^{ij}L_{\text{measstd}} - \overline{jL_{\text{measstd}}} \right)^2$	$f_e = (n_3 - 1) \cdot n_4$	$V_e = \frac{S_e}{f_e}$	$u_{\text{measstd,L,rep}}^2$
$S = \sum_{i=1}^{n_3} \sum_{j=1}^{n_4} \left( {}^{ij}L_{\text{measstd}} - \overline{\overline{L_{\text{measstd}}}} \right)^2$	$f = n_3 \cdot n_4 - 1$		
$u_{\text{measstd,L,rep}}^2 = V_e$			
$u_{\text{measstd,L,geo}}^2 = \frac{V_A - V_e}{n_3}$			

Example:  $E_S$  and  $u_S$  evaluation.

	Orientation 1 (X axis direction)	Orientation 2 (Y axis direction)	Orientation 3 (Z axis direction)
Repeat 1/mm	100.0019	100.0020	100.0008
Repeat 2/mm	100.0016	100.0009	100.0010
Repeat 3/mm	100.0020	100.0010	100.0012
$\overline{jL_{\text{measstd}}}$ /mm	100.0018	100.0013	100.0010
$\overline{\overline{L_{\text{measstd}}}}$	100.0014 mm		
$L_{\text{calstd}}$	100.0014 mm		
$E_S$	0.0000 mm		
$U_{\text{calstd,L}}$	0.0004 mm		

S/mm <sup>2</sup>	DOF	Variance/mm <sup>2</sup>	Expectation of
$S_A = \sum_{i=1}^{n_3} \sum_{j=1}^{n_4} \left( \overline{jL_{\text{measstd}}} - \overline{L_{\text{measstd}}} \right)^2 = 0.000\ 001\ 1$	$f_A = n_4 - 1 = 2$	$V_A = \frac{S_A}{f_A} = 0.000\ 000\ 5$	$u_{\text{measstd,L,rep}}^2 + n_3 \cdot u_{\text{measstd,L,geo}}^2$
$S_e = \sum_{i=1}^{n_3} \sum_{j=1}^{n_4} \left( {}^{ij}L_{\text{measstd}} - \overline{jL_{\text{measstd}}} \right)^2 = 0.000\ 000\ 9$	$f_e = (n_3 - 1) \cdot n_4 = 6$	$V_e = \frac{S_e}{f_e} = 0.000\ 000\ 2$	$u_{\text{measstd,L,rep}}^2$
$S_e = \sum_{i=1}^{n_3} \sum_{j=1}^{n_4} \left( {}^{ij}L_{\text{measstd}} - \overline{jL_{\text{measstd}}} \right)^2 = 0.000\ 002\ 0$	$f = n_3 \cdot n_4 - 1 = 8$		
$u_{\text{measstd,L,rep}}^2 = V_e = 0.000\ 000\ 2\ \text{mm}^2$			
$u_{\text{measstd,L,geo}}^2 = \frac{V_A - V_e}{n_3} = 0.000\ 000\ 1\ \text{mm}^2$			
$u_S^2 = \left( \frac{U_{\text{calstd,L}}}{2} \right)^2 + \frac{u_{\text{measstd,L,rep}}^2}{n_3} + \frac{u_{\text{measstd,L,geo}}^2}{n_4} = \left[ \left( \frac{0.0004}{2} \right)^2 + \frac{0.000\ 000\ 2}{3} + \frac{0.000\ 000\ 1}{3} \right] \text{mm}^2 = 0.000\ 000\ 1\ \text{mm}^2$			

**Example: Distance of two inner cylinders.**

Let us apply the above evaluation to a complete example: the distance of the centres of two inner cylinders. The measurements are done with a single stylus in each orientation (see Figure 6).

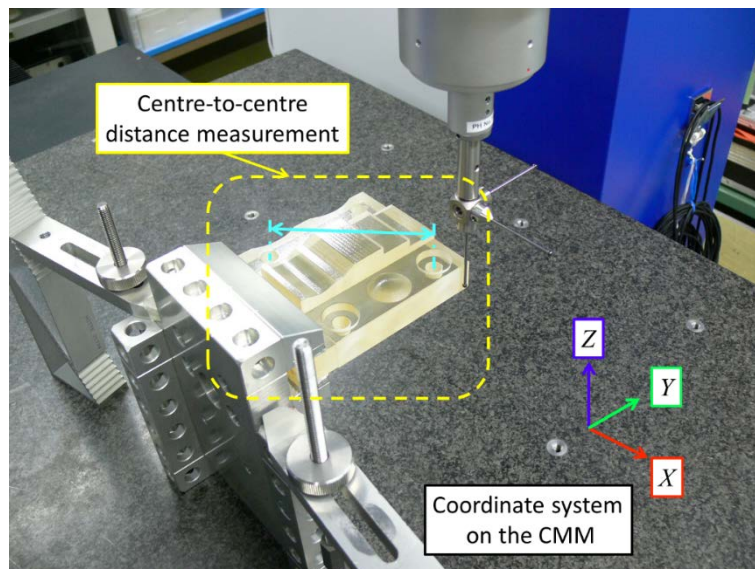


Figure 6 Measurement of the distance of two cylinders centres (home position).

Some of uncertainty components are not relevant in this measurement:

$E_D = 0$  (monodirectional probing)

$E_{\text{PrbLoc}}$  (a single stylus is used in each orientation)



$$u_{\text{geo} \times \text{dist}}^2 \text{ (not a form measurement)}$$

The effect of the temperature variation is omitted in this example.

As the CMM used is extremely high quality and well temperature compensated, the scale error derived from the measurements of a standard of length resulted null,  $E_S = 0$ . Its variance—evaluated as in the previous example—resulted  $u_S^2 = 0.000\ 0000\ 1\ \text{mm}^2$ .

Example: distance of the centres of two inner cylinders.

	Orientation 1 (home position)	Orientation 2	Orientation 3	Orientation 4
Repeat 1/mm	98.9892	98.9891	98.9894	98.9898
Repeat 2/mm	98.9889	98.9889	98.9891	98.9896
Repeat 3/mm	98.9890	98.9889	98.9891	98.9895
$\overline{j}y/\text{mm}$	98.9890	98.9890	98.9892	98.9896
$\overline{y}$	98.9892 mm			
$S/\text{mm}^2$	DOF		Variance/ $\text{mm}^2$	Expectation of
$S_A = \sum_{i=1}^{n_1} \sum_{j=1}^{n_2} (j\overline{y} - \overline{j}y)^2 = 0.000\ 000\ 7$	$f_A = n_2 - 1 = 3$		$V_A = \frac{S_A}{f_A} = 0.000\ 000\ 2$	$u_{\text{rep}}^2 + n_1 u_{\text{geo}}^2 = u_{\text{rep}}^2 + 3u_{\text{geo}}^2$
$S_e = \sum_{i=1}^{n_1} \sum_{j=1}^{n_2} (ijy - j\overline{j}y)^2 = 0.000\ 000\ 2$	$f_e = (n_1 - 1) \cdot n_2 = 8$		$V_e = \frac{S_e}{f_e} = 0.000\ 000\ 0$	$u_{\text{rep}}^2$
$S = \sum_{i=1}^{n_1} \sum_{j=1}^{n_2} (ijy - \overline{j}y)^2 = 0.000\ 000\ 9$	$f = n_1 \cdot n_2 - 1 = 11$			
$u_{\text{rep}}^2 = V_e = 0.000\ 000\ 0\ \text{mm}^2$				
$u_{\text{geo}}^2 = \frac{(V_A - V_e)}{n_1} = 0.000\ 000\ 1\ \text{mm}^2$				
$E_S = 0.0000\ \text{mm}^2$		$u_S^2 = 0.000\ 000\ 1\ \text{mm}^2$		
(details omitted for brevity; see previous example)				
$U = k \cdot \sqrt{ E_S ^2 + \frac{u_{\text{rep}}^2}{n_1} + \frac{u_{\text{geo}}^2}{n_2} + u_S^2}$ $= 3 \sqrt{0.000\ 000\ 0 + \frac{0.000\ 000\ 0}{3} + \frac{0.000\ 000\ 1}{4} + 0.000\ 000\ 1\ \text{mm}} = 0.0012\ \text{mm}$				
if the scale error is not corrected for, $\overline{y}$ , or				

$$U = k \cdot \sqrt{\frac{u_{\text{rep}}^2}{n_1} + \frac{u_{\text{geo}}^2}{n_2} + u_S^2} = 3 \sqrt{\frac{0.000\ 000\ 0}{3} + \frac{0.000\ 000\ 1}{4} + 0.000\ 000\ 1 \text{ mm}} = 0.0012 \text{ mm}$$

if the scale error is corrected for,  $\bar{y} - E_S$ .

### 3.3.3 Evaluation of $u_D$

The uncertainty due to the average probe size error,  $u_D$ , is derived from the following equation;

$$u_D^2 = \left(\frac{U_{\text{calstd,D}}}{2}\right)^2 + \frac{u_{\text{measstd,D,rep}}^2}{n_5} + \frac{u_{\text{measstd,D,geo}}^2}{n_6},$$

Where  $U_{\text{calstd,D}}$  is the expanded calibration uncertainty ( $k = 2$ ) of the test sphere as reported in its calibration certificate, and  $u_{\text{measstd,D,rep}}$  and  $u_{\text{measstd,D,geo}}$ , are evaluated with the ANOVA approach (see Table 12).

Table 7 Evaluation of  $u_{\text{measstd,D,rep}}$  and  $u_{\text{measstd,D,geo}}$  (ANOVA).

$\overline{jD_{\text{measstd}}} = \frac{1}{n_5} \sum_{i=1}^{n_5} ijD_{\text{measstd}}$			
$\overline{D_{\text{measstd}}} = \frac{1}{n_5 n_6} \sum_{i=1}^{n_5} \sum_{j=1}^{n_6} ijD_{\text{measstd}}$			
Sum of squares	Degrees of freedom (DOF)	Variance	Expectation of
$S_A = \sum_{i=1}^{n_5} \sum_{j=1}^{n_6} \left( \overline{jD_{\text{measstd}}} - \overline{D_{\text{measstd}}} \right)^2$	$f_A = n_6 - 1$	$V_A = \frac{S_A}{f_A}$	$u_{\text{measstd,L,rep}}^2 + n_5 \cdot u_{\text{measstd,L,geo}}^2$
$S_e = \sum_{i=1}^{n_5} \sum_{j=1}^{n_6} \left( ijD_{\text{measstd}} - \overline{jD_{\text{measstd}}} \right)^2$	$f_e = (n_5 - 1) \cdot n_6$	$V_e = \frac{S_e}{f_e}$	$u_{\text{measstd,L,rep}}^2$
$S = \sum_{i=1}^{n_5} \sum_{j=1}^{n_6} \left( ijD_{\text{measstd}} - \overline{D_{\text{measstd}}} \right)^2$	$f = n_5 \cdot n_6 - 1$		
$u_{\text{measstd,D,rep}}^2 = V_e$			
$u_{\text{measstd,D,geo}}^2 = \frac{V_A - V_e}{n_3}$			

Example:  $E_D$  and  $u_D$  evaluation.

	Probe 1	Probe 2	Probe 3
Repeat 1/mm	29.9869	29.9861	29.9865
Repeat 2/mm	29.9868	29.9860	29.9866
Repeat 3/mm	29.9868	29.9861	29.9865
$\overline{^j D_{\text{measstd}}}$ /mm	29.9868	29.9861	29.9865
$\overline{\overline{D_{\text{measstd}}}}$	29.9865 mm		
$D_{\text{calstd}}$	29.9863 mm		
$D_L$	0.0002 mm		
$U_{\text{calstd,D}}$	0.000 15 mm		
S/mm <sup>2</sup>	DOF	Variance/mm <sup>2</sup>	Expectation of
$S_A = \sum_{i=1}^{n_5} \sum_{j=1}^{n_6} \left( \overline{^j D_{\text{measstd}}} - \overline{\overline{D_{\text{measstd}}}} \right)^2 = 0.000\ 000\ 8$	$f_A = n_4 - 1 = 2$	$V_A = \frac{S_A}{f_A} = 0.000\ 000\ 4$	$u_{\text{measstd,L,rep}}^2 + n_5 \cdot u_{\text{measstd,L,geo}}^2$
$S_e = \sum_{i=1}^{n_5} \sum_{j=1}^{n_6} \left( {}^{ij} D_{\text{measstd}} - \overline{^j D_{\text{measstd}}} \right)^2 = 0.000\ 000\ 0$	$f_e = (n_5 - 1) \cdot n_6 = 6$	$V_e = \frac{S_e}{f_e} = 0.000\ 000\ 0$	$u_{\text{measstd,D,rep}}^2$
$S_e = \sum_{i=1}^{n_5} \sum_{j=1}^{n_6} \left( {}^{ij} D_{\text{measstd}} - \overline{\overline{^j D_{\text{measstd}}}} \right)^2 = 0.000\ 000\ 8$	$f = n_5 \cdot n_6 - 1 = 8$		
$u_{\text{measstd,D,rep}}^2 = V_e = 0.000\ 000\ 0\ \text{mm}^2$			
$u_{\text{measstd,D,geo}}^2 = \frac{V_A - V_e}{n_5} = 0.000\ 000\ 1\ \text{mm}^2$			
$u_D^2 = \left( \frac{U_{\text{calstd,D}}}{2} \right)^2 + \frac{u_{\text{measstd,D,rep}}^2}{n_5} + \frac{u_{\text{measstd,D,geo}}^2}{n_6}$ $= \left[ \left( \frac{0.000\ 15}{2} \right)^2 + \frac{0.000\ 000\ 0}{3} + \frac{0.000\ 000\ 1}{3} \right] \text{mm}^2 = 0.000\ 000\ 1\ \text{mm}^2$			

Example: the diameter of an inner cylinder.

Let us apply the above evaluation to another complete example: the diameter of an inner cylinder. The measurements are done with a single stylus in each orientation (see Figure 7).

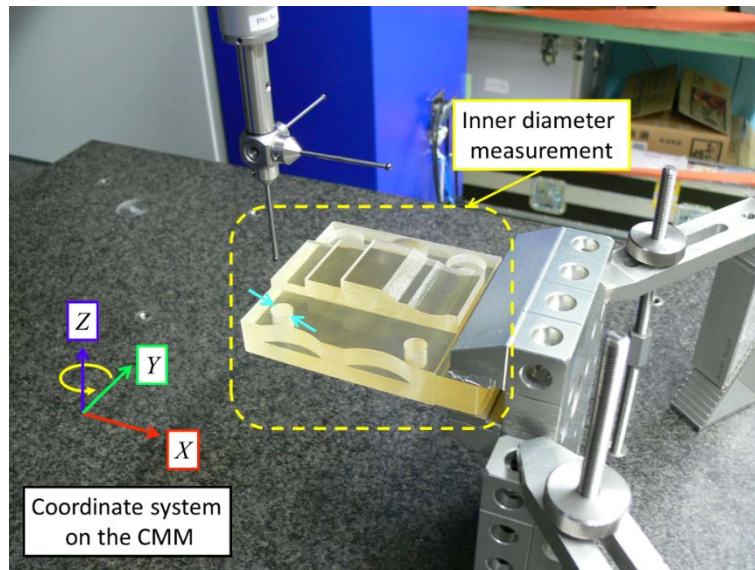


Figure 7 Measurement of the diameter of an inner cylinder (Orientation 4).

Some of uncertainty components are not relevant in this measurement:

$E_{PrbLoc}$  (a single stylus is used in each orientation)

$u_{geo \times dist}^2$  (not a form measurement)

The effect of the temperature variation is omitted in this example.

As in the previous complete example, some evaluation details (namely of  $E_S, u_S, E_D, u_D$ ) are omitted for brevity.

Example: diameter of an inner cylinder.

	Orientation 1 (home position)	Orientation 2	Orientation 3	Orientation 4
Repeat 1/mm	10.1759	10.1766	10.1787	10.1741
Repeat 2/mm	10.1767	10.1770	10.1794	10.1751
Repeat 3/mm	10.1770	10.1767	10.1794	10.1756
$^j\bar{y}/\text{mm}$	10.1765	10.1768	10.1792	10.1749
$\bar{y}$	10.1769 mm			

S/mm <sup>2</sup>	DOF	Variance/mm <sup>2</sup>	Expectation of
$S_A = \sum_{i=1}^{n_1} \sum_{j=1}^{n_2} (j\bar{y} - \bar{y})^2 =$ $= 0.000\ 027\ 4$	$f_A = n_2 - 1 = 3$	$V_A = \frac{S_A}{f_A} =$ $= 0.000\ 009\ 1$	$u_{\text{rep}}^2 + n_1 u_{\text{geo}}^2 =$ $= u_{\text{rep}}^2 + 3u_{\text{geo}}^2$
$S_e = \sum_{i=1}^{n_1} \sum_{j=1}^{n_2} (ijy - j\bar{y})^2 =$ $= 0.000\ 002\ 2$	$f_e = (n_1 - 1) \cdot n_2 = 8$	$V_e = \frac{S_e}{f_e} =$ $= 0.000\ 000\ 3$	$u_{\text{rep}}^2$
$S = \sum_{i=1}^{n_1} \sum_{j=1}^{n_2} (ijy - \bar{y})^2 =$ $= 0.000\ 029\ 7$	$f = n_1 \cdot n_2 - 1 = 11$		
$u_{\text{rep}}^2 = V_e = 0.000\ 000\ 3\ \text{mm}^2$			
$u_{\text{geo}}^2 = \frac{(V_A - V_e)}{n_1} = 0.000\ 003\ 0\ \text{mm}^2$			
$E_S = 0.0000\ \text{mm}$		$u_S^2 = 0.000\ 000\ 1\ \text{mm}^2$	
(details omitted for brevity)			
$ E_D ^2 = 0.000\ 000\ 6\ \text{mm}^2$		$u_D^2 = 0.000\ 000\ 3\ \text{mm}^2$	
(details omitted for brevity)			
$U = k \cdot \sqrt{ E_S ^2 +  E_D ^2 + \frac{u_{\text{rep}}^2}{n_1} + \frac{u_{\text{geo}}^2}{n_2} + u_S^2 + u_D^2}$ $= 3 \sqrt{0.000\ 000\ 0 + 0.000\ 000\ 6 + \frac{0.000\ 000\ 3}{3} + \frac{0.000\ 003\ 0}{4} + 0.000\ 000\ 1 + 0.000\ 000\ 3}\ \text{mm}$ $= 0.0042\ \text{mm}$ <p>if neither the scale nor the probe size error are corrected for, <math>\bar{y}</math>, or</p> $U = k \cdot \sqrt{ E_D ^2 + \frac{u_{\text{rep}}^2}{n_1} + \frac{u_{\text{geo}}^2}{n_2} + u_S^2 + u_D^2}$ $= 3 \sqrt{0.000\ 000\ 6 + \frac{0.000\ 000\ 3}{3} + \frac{0.000\ 003\ 0}{4} + 0.000\ 000\ 1 + 0.000\ 000\ 3}\ \text{mm} = 0.0041\ \text{mm}$ <p>if the probe size error only in corrected for, <math>\bar{y} + E_D</math>, or</p> $U = k \cdot \sqrt{\frac{u_{\text{rep}}^2}{n_1} + \frac{u_{\text{geo}}^2}{n_2} + u_S^2 + u_D^2}$ $= 3 \sqrt{\frac{0.000\ 000\ 3}{3} + \frac{0.000\ 003\ 0}{4} + 0.000\ 000\ 1 + 0.000\ 000\ 3}\ \text{mm} = 0.0034\ \text{mm}$ <p>if the both the scale and the probe size error are corrected for, <math>\bar{y} - E_S + E_D</math>.</p>			

### 3.3.4 Evaluation of $u_{PrbLoc}$

The uncertainty of the average probe location error,  $u_{PrbLoc}$ , is derived from the following equation:

$$u_{PrbLoc}^2 = \frac{|E_{PrbLoc}|^2}{12}$$

### 3.3.5 Evaluation of $u_{geo \times dist}$

The local distances of the measured points to the ideal surface are measured. The form error is obtained as the range of these distances. This uncertainty component estimates the uncertainty of the local form deviations,  $U_{Point}$ .

The uncertainty of the overall form deviations is evaluated as  $\sqrt{2}U_{Point}$ , as the form error is the difference of the extreme values (range) of the local deviations [8]<sup>9</sup>.  $n_7$  points are chosen to evaluate the uncertainty contributor  $u_{geo \times dist}$ . The points may be those already used to evaluate the form deviation, or sampled additionally for the purpose.

The measured values  $ijk_y$  involved in this evaluation are summarised in Table 10, with  $j = 1 \dots n_2$  indicating the orientations,  $i = 1 \dots n_1$  the measurement repeats within the same orientation, and  $k = 1 \dots n_7$  the measurement points in the same repetition.

Table 8 Summary of measured points for the evaluation of  $u_{geo \times dist}$ .

	Orientation 1 (home position)	Orientation 2	Orientation 3	Orientation 4
Repeat 1	$1^{11}_y$	$1^{21}_y$	$1^{31}_y$	$1^{41}_y$
	☒	☒	☒	☒
	$1^{1n_7}_y$	$1^{2n_7}_y$	$1^{3n_7}_y$	$1^{4n_7}_y$
Repeat 2	$2^{11}_y$	$2^{21}_y$	$2^{31}_y$	$2^{41}_y$
	☒	☒	☒	☒
	$2^{1n_7}_y$	$2^{2n_7}_y$	$2^{3n_7}_y$	$2^{4n_7}_y$
Repeat 3	$3^{11}_y$	$3^{21}_y$	$3^{31}_y$	$3^{41}_y$
	☒	☒	☒	☒
	$3^{1n_7}_y$	$3^{2n_7}_y$	$3^{3n_7}_y$	$3^{4n_7}_y$

$u_{rep}$ ,  $u_{geo}$  and  $u_{geo \times dist}$  are evaluated as summarised in Table 9. The ANOVA approach is two-level in this case, as the level of the sampled points adds on that of the orientations.

<sup>9</sup> Given a set of spastically independent random variables  $\xi_i$ ,  $i \in [1 \dots p]$ , the uncertainty of its range  $r = \xi_{max} - \xi_{min}$  is not simply the quadratic sum of the uncertainties of the maximum and minimum values, as the equation may suggests. In fact, the range is a case of order statistics, that is, sorting the values in the set to get the minimum and maximum values at the extremes alters the simplistic quadratic summation. This alteration decreases asymptotically with  $p$ . In the usual case of a reasonable number of points for a form measurement, the simple quadratic sum is a good estimate of the range uncertainty, particularly in coordinate metrology where the many other difficulties make this subtlety negligible.

This ANOVA exercise evaluates not only  $u_{\text{geo}\times\text{dist}}$  but  $u_{\text{rep}}$  and  $u_{\text{geo}}$  as well.  $u_{\text{dist}}$  (the standard deviation of the distribution of the point distances to the surface) is also evaluated but not added explicitly because already accounted for.

Table 9 Evaluation of  $u_{\text{rep}}$ ,  $u_{\text{geo}}$  and  $u_{\text{geo}\times\text{dist}}$  (ANOVA).

${}^{jk}\bar{y} = \frac{1}{n_1} \sum_{i=1}^{n_1} {}^{ijk}y$			
${}^j\bar{\bar{y}} = \frac{1}{n_1 n_7} \sum_{i=1}^{n_1} \sum_{k=1}^{n_7} {}^{ijk}y$			
${}^k\bar{\bar{y}} = \frac{1}{n_1 n_2} \sum_{i=1}^{n_1} \sum_{j=1}^{n_2} {}^{ijk}y$			
$\bar{\bar{\bar{y}}} = \frac{1}{n_1 n_2 n_7} \sum_{i=1}^{n_1} \sum_{j=1}^{n_2} \sum_{k=1}^{n_7} {}^{ijk}y$			
Sum of squares	Degrees of freedom (DOF)	Variance	Expectation of
$S_A = \sum_{i=1}^{n_1} \sum_{j=1}^{n_2} \sum_{k=1}^{n_7} ({}^j\bar{\bar{y}} - \bar{\bar{\bar{y}}})^2$	$f_A = n_2 - 1$	$V_A = \frac{S_A}{f_A}$	$n_1 n_7 u_{\text{geo}}^2 + n_1 u_{\text{geo}\times\text{dist}}^2 + u_{\text{rep}}^2$
$S_B = \sum_{i=1}^{n_1} \sum_{j=1}^{n_2} \sum_{k=1}^{n_7} ({}^k\bar{\bar{y}} - \bar{\bar{\bar{y}}})^2$	$f_B = n_7 - 1$	$V_e = \frac{S_e}{f_e}$	$n_1 n_2 u_{\text{dist}}^2 + n_1 u_{\text{geo}\times\text{dist}}^2 + u_{\text{rep}}^2$
$S_{A\times B} = \sum_{i=1}^{n_1} \sum_{j=1}^{n_2} \sum_{k=1}^{n_7} ({}^{jk}\bar{y} - {}^j\bar{\bar{y}} - {}^k\bar{\bar{y}} + \bar{\bar{\bar{y}}})^2$	$f_{A\times B} = (n_2 - 1)(n_7 - 1)$	$V_{A\times B} = \frac{S_{A\times B}}{f_{A\times B}}$	$n_1 u_{\text{geo}\times\text{dist}}^2 + u_{\text{rep}}^2$
$S_e = \sum_{i=1}^{n_1} \sum_{j=1}^{n_2} \sum_{k=1}^{n_7} ({}^{ijk}y - {}^{jk}\bar{y})^2$	$f_e = (n_1 - 1)n_2 n_7$	$V_e = \frac{S_e}{f_e}$	$u_{\text{rep}}^2$
$S = \sum_{i=1}^{n_1} \sum_{j=1}^{n_2} \sum_{k=1}^{n_7} ({}^{ijk}y - \bar{\bar{\bar{y}}})^2$	$f = n_1 n_2 n_7 - 1$		

$u_{\text{rep}}^2 = V_e$
$u_{\text{geo} \times \text{dist}}^2 = \frac{V_{A \times B} - V_e}{n_1}$
$u_{\text{dist}}^2 = \frac{V_A - V_{A \times B}}{n_7}$ (not added to the final uncertainty, as already accounted for)
$u_{\text{geo}}^2 = \frac{V_B - V_e}{(n_2 - 1)n_7}$

Example: flatness measurement.

The following example shows the uncertainty evaluation for a flatness measurement. The plane is measured with a single stylus in each orientation (see Figure 8). Each plane is measured over  $n_7 = 12$  points.

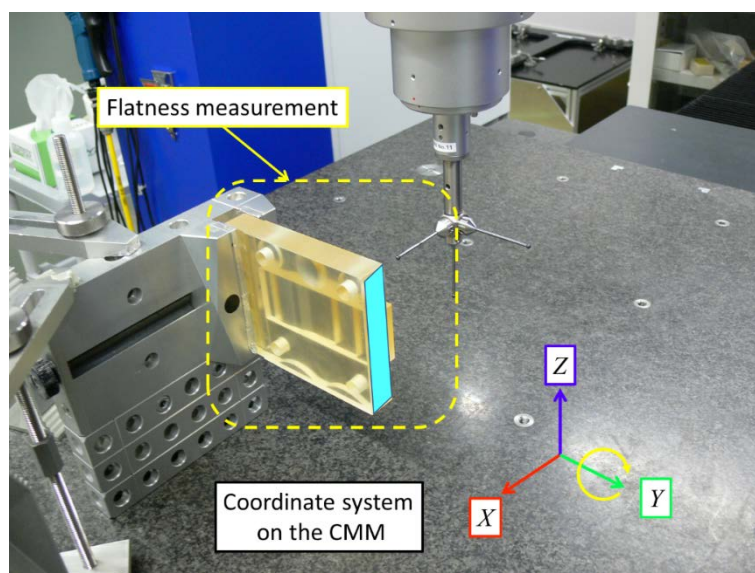


Figure 8 Measurement of flatness (Orientation 3).

Example: flatness measurement.

	Orientation 1 (home position)	Orientation 2	Orientation 3	Orientation 4
Repeat 1/mm	0.0029	0.0026	0.0007	0.0009
	⊗	⊗	⊗	⊗
	-0.0019	-0.0021	-0.0012	-0.0008
Repeat 2/mm	0.0020	0.0021	0.0007	0.0003
	⊗	⊗	⊗	⊗



	-0.0017	-0.0019	-0.0013	-0.0008
Repeat 3/mm	0.0015	0.0019	0.0008	0.0000
	☒	☒	☒	☒
	-0.0015	-0.0019	-0.0012	-0.0007
$\bar{y}$	0.0000 mm			
S/mm <sup>2</sup>	DOF	Variance/mm <sup>2</sup>	Expectation of	
$S_A = 0.000\ 200\ 58$	$f_A = n_7 - 1 = 11$	$V_A = \frac{S_A}{f_A} = 0.000\ 018\ 23$	$n_1 n_7 u_{\text{geo}}^2 + n_1 u_{\text{geo} \times \text{dist}}^2 + u_{\text{rep}}^2 = 36 u_{\text{geo}}^2 + 3 u_{\text{geo} \times \text{dist}}^2 + u_{\text{rep}}^2$	
$S_B = 0.000\ 000\ 07$	$f_B = n_2 - 1 = 3$	$V_B = \frac{S_B}{f_B} = 0.000\ 000\ 02$	$n_1 n_2 u_{\text{dist}}^2 + n_1 u_{\text{geo} \times \text{dist}}^2 + u_{\text{rep}}^2 = 12 u_{\text{dist}}^2 + 3 u_{\text{geo} \times \text{dist}}^2 + u_{\text{rep}}^2$	
$S_{A \times B} = 0.000\ 014\ 11$	$f_{A \times B} = (n_2 - 1)(n_7 - 1) = 33$	$V_{A \times B} = \frac{S_{A \times B}}{f_{A \times B}} = 0.000\ 000\ 43$	$n_1 u_{\text{geo} \times \text{dist}}^2 + u_{\text{rep}}^2 = 3 u_{\text{geo} \times \text{dist}}^2 + u_{\text{rep}}^2$	
$S_e = 0.000\ 027\ 5$	$f_e = (n_1 - 1)n_2 n_7 = 96$	$V_e = \frac{S_e}{f_e} = 0.000\ 000\ 03$	$u_{\text{rep}}^2$	
$S = 0.000\ 217\ 51$	$f = n_1 n_2 n_7 - 1 = 143$			
$u_{\text{rep}}^2 = V_e = 0.000\ 000\ 03\ \text{mm}^2$				
$u_{\text{geo} \times \text{dist}}^2 = \frac{V_{A \times B} - V_e}{n_1} = 0.000\ 000\ 13\ \text{mm}^2$				
$u_{\text{dist}}^2 = \frac{V_A - V_{A \times B}}{n_7} = 0.000\ 001\ 5\ \text{mm}^2$ (not added to the final uncertainty, as already accounted for)				
$u_{\text{geo}}^2 = \frac{V_B - V_e}{(n_2 - 1)n_7} = -2.8 \times 10^{-10}\ \text{mm}^2 \rightarrow 0$ (forced to zero because $u_{\text{geo}}$ is imaginary due to rounding [16])				
$U = \sqrt{2}k \sqrt{\frac{u_{\text{rep}}^2}{n_1} + \frac{u_{\text{geo}}^2}{n_2} + u_{\text{geo} \times \text{dist}}^2} = 3\sqrt{2} \sqrt{\frac{0.000\ 000\ 03}{3} + \frac{0}{4} + 0.000\ 000\ 13}\ \text{mm} = 0.0016\ \text{mm}$				

### 3.3.6 Evaluation of $u_{\text{temp}}$

The procedure described above is insensitive to thermal errors: repeats and reversals would all be affected by the same thermal error<sup>10</sup> and the ANOVA analysis would be ineffective. As a consequence, this uncertainty component is evaluated separately, typically *a priori* (type B). Strictly speaking, this is not part of the *a posteriori* (type A) evaluation method described in this document. It is briefly mentioned here for two reasons:

1. Thermal effects are usually extremely important in dimensional measurements and at least a reminder to account for them is essential.
2. This method is intended to give input to a future ISO 15530-2. In this view, this uncertainty component *must* be mentioned, even if evaluated *a priori*, to give the standard readers guidance and not to mislead them in forgetting about it.

The evaluation procedure for  $u_{\text{temp}}$  is taken from section A.9 of the ISO/DTS 15530-2 [8] with no modifications. This uncertainty component is a combination of the uncertainty due to the temperatures of workpiece and CMM scales and to their CTE (*Coefficient of Thermal Expansion*). This evaluation is rather typical in dimensional metrology. Further general guidance is found in [17].

## 3.4 Special cases

### 3.4.1 Poor available information

In evaluating the uncertainty in form measurement (see 3.3.5),  $u_{\text{rep}}$ ,  $u_{\text{geo}}$  and  $u_{\text{geo} \times \text{dist}}$  are evaluated from the local form deviations of all probed points. This information is available to the CMM software and stored in its internal memory. Unfortunately, many CMM software interfaces do not make this information available to the user. The information they disclose is limited to the two values of local peak ( $P$ ) and valley ( $V$ ) deviations, or even to the single unsigned peak-to-valley value ( $W = P - V$ ).

In such cases, the maximum entropy principle is followed: the unknown distribution of local form deviations is assumed to be the one that maximizes the information entropy.

#### 3.4.1.1 Two values, peak ( $P$ ) and valley ( $V$ )

The peak and valley values yielded along the procedure are arranged as shown in Table 10.

Table 10 Summary of form measurement results.

	Orientation 1 (home position)	Orientation 2	Orientation 3	Orientation 4
Repeat 1	$^{11}V$	$^{12}V$	$^{13}V$	$^{14}V$
	$^{11}P$	$^{12}P$	$^{13}P$	$^{14}P$
Repeat 2	$^{21}V$	$^{22}V$	$^{23}V$	$^{24}V$
	$^{21}P$	$^{22}P$	$^{23}P$	$^{24}P$
Repeat 3	$^{31}V$	$^{32}V$	$^{33}V$	$^{34}V$
	$^{31}P$	$^{32}P$	$^{33}P$	$^{34}P$

<sup>10</sup> This is when the temperature is uniform in time and space. When it is not, additional errors are introduced, which are not properly captured by the experimental procedure.

$u_{rep}$ ,  $u_{geo}$  and  $u_{geo,dist}$  can be evaluated as described in 3.3 with  $n_7 = 2$  regardless of the actual number of measured points<sup>11</sup>.

### 3.4.1.2 Single unsigned peak-to-valley value, $W$

When the value  $W$  only is available (Table 11), then  $n_7 = 1$  and the ANOVA equations in Table 9 fail as the number of some degrees of freedom drops to zero: at least two values are needed. The total form error is then split arbitrarily in two peak and valley values such as their difference is  $W$ .

Following the maximum entropy principle, the peak and valley values are simply taken symmetrically about zero, that is,  $P = -V$ . Table 12 results.

Table 11 Summary of form measurement results.

	Orientation 1 (home position)	Orientation 2	Orientation 3	Orientation 4
Repeat 1	$^{11}W$	$^{12}W$	$^{13}W$	$^{14}W$
Repeat 2	$^{21}W$	$^{22}W$	$^{23}W$	$^{24}W$
Repeat 3	$^{31}W$	$^{32}W$	$^{33}W$	$^{34}W$

Table 12 Modified summary of form measurement results

	Orientation 1 (home position)	Orientation 2	Orientation 3	Orientation 4
Repeat 1	$-^{11}W/2$	$-^{12}W/2$	$-^{13}W/2$	$-^{14}W/2$
	$^{11}W/2$	$^{12}W/2$	$^{13}W/2$	$^{14}W/2$
Repeat 2	$-^{21}W/2$	$-^{22}W/2$	$-^{23}W/2$	$-^{24}W/2$
	$^{21}W/2$	$^{22}W/2$	$^{23}W/2$	$^{24}W/2$
Repeat 3	$-^{31}W/2$	$-^{32}W/2$	$-^{33}W/2$	$-^{34}W/2$
	$^{31}W/2$	$^{32}W/2$	$^{33}W/2$	$^{34}W/2$

$u_{rep}$ ,  $u_{geo}$  and  $u_{geo,dist}$  can be evaluated as described in 3.3 with  $n_7 = 2$  regardless of the actual number of measured points.

<sup>11</sup> The derivation of data is expected to lead to overestimation for two reasons:

1. The number of points is not sufficient to neglect the effect of sorting the values in each set  $ij$  (see footnote 9);
2. The maximum entropy principle would lead to assuming the missing populations of local form deviations as uniform in the intervals  $[^{ij}V, ^{ij}P]$ . This would lead to standard uncertainties of  $(^{ij}V - ^{ij}P)/\sqrt{12}$ , whereas the equivalent standard deviations based on the extreme values only amount to  $(^{ij}V - ^{ij}P)/\sqrt{2}$ .

These aspects were not investigated in depth and may lead in future to a more favourable evaluation of the uncertainty.

### 3.4.2 Extension to scanning

When a form measurement is done in scanning probing mode, the number of sampled points is affected by the scanning parameters such as the scanning speed and the sampling point density. Even if they are kept the same throughout the measurement procedure, different repeats may result in different numbers of sampled points, particularly when the points are very many. Arranging them in tables such as Table 8 may lead to uneven columns: the correspondence among related values is lost.

To overcome this problem, a modification of the method described in 3.3.5 is required.

For a precise uncertainty estimation, the ANOVA analysis applies with unequal sampling sizes. In this case,  $u_{\text{geo},x,\text{dist}}$  is removed from the uncertainty evaluation because of the lack of correspondence among points in the measurement sequence.

For a practical uncertainty estimation, the ANOVA analysis with the maximum entropy model applies. The set of sampled points of any repeat is replaced by its maximum and minimum values, and the procedure described in 3.4.1 applies, including ( $u_{\text{geo},x,\text{dist}}$ ).

### 3.4.3 Prismatic tolerance zones

Derived features (such as a median line of a cylinder) may be subject to tolerances with prismatic tolerance zones. They possess a defined axis and all their cross sections with any plane orthogonal to the axis are identical. The cross sections can be either rectangular or circular. An extreme case of the former is when a dimensions of the rectangle goes to infinite, that is, when the rectangle degenerates to a strip and the prism to the space between two parallel planes.

Prismatic tolerance zones with rectangular cross-section [18]<sup>12</sup> control form deviations along two perpendicular directions aligned to the rectangle (secondary datum). The measurands are then two: the local form deviations along each of such directions. The local form deviations are signed and the uncertainty evaluation procedures described either in 3.3 (complete evaluation) or in 3.4.1.1 or 3.4.1.2 (reduced evaluation) are applicable.

In prismatic tolerance zones with circular cross-section (cylinders) [18]<sup>13</sup>, the local form deviations are the distance to the cylinder axis, which is unsigned. The maximum entropy approach then applies, very similarly to 3.4.1.2. The only difference is that Table 12 therein is modified to Table 13:

---

<sup>12</sup> For example, this is the case of a double perpendicularity tolerance of a same feature (such as the median line of a cylinder) with reference to a datums system that constrains all three orientation angles (see [18] Figure 132). The tolerances in the two directions orthogonal to the primary datum are independent, generating a rectangular cross-section tolerance zone.

<sup>13</sup> For example, this is the case of a perpendicularity tolerance with a  $\varnothing$  sign in the callout, of a feature (such as the median line of a cylinder) with reference to (at least) a primary datum constraining two orientation angles (see [18] Figure 134).

Table 13 Modified summary of form measurement results

	Orientation 1 (home position)	Orientation 2	Orientation 3	Orientation 4
Repeat 1	$-^{11}W$	$-^{12}W$	$-^{13}W$	$-^{14}W$
	$^{11}W$	$^{12}W$	$^{13}W$	$^{14}W$
Repeat 2	$-^{21}W$	$-^{22}W$	$-^{23}W$	$-^{24}W$
	$^{21}W$	$^{22}W$	$^{23}W$	$^{24}W$
Repeat 3	$-^{31}W$	$-^{32}W$	$-^{33}W$	$-^{34}W$
	$^{31}W$	$^{32}W$	$^{33}W$	$^{34}W$

When the form deviation is signed (as in 3.4.1.2), the maximum entropy approach leads to attributing half value to the positive and half to the negative range. Let us reduce the case of unsigned form deviations to the previous case of signed ones.

Let us define a coordinate system having the  $z$  axis coincident with the axis of the cylinder (the tolerance zone) and the  $xz$  plane chosen arbitrary. Let us define positive directions of the  $z$  and  $x$  axes arbitrarily. Let us define the operation *roto-projection* as follows: given a point in space, rotate it clockwise about  $z$  until it hits the  $xz$  plane; the hit point is the roto-projected point. Let us rot-project all measured points. The roto-projected points are still off the  $z$  axis of the same amount as the original ones, but all lay in the  $xz$  plane. The local form deviations are expressed with the coordinates  $x$  only, which are signed<sup>14</sup>. The information that the maximum local deviation is  $W$ —i.e. the cylinder *radius*—is reflected to the coordinate range  $[-W, W]$ —the cylinder *diameter*.

### 3.4.3.1 Straightness

The toleranced feature controlled by a straightness tolerance can be either 2D<sup>15</sup> or 3D<sup>16</sup>.

In the former case, the tolerance zone is the strip in the intersection plane between two parallel lines. The local form deviations are signed as long as a positive direction is defined in the intersection plane. A typical choice is positive for points laying in air, negative for points laying in the material. The uncertainty evaluation procedures described either in 3.3 (complete evaluation) or in 3.4.1.1 or 3.4.1.2 (reduced evaluation) are applicable.

In the latter case, the tolerance zone has a prismatic form, either a parallelepiped or a cylinder. See 3.4.3 above.

### 3.4.3.2 Position tolerance

the tolerance zone has a prismatic form, either a parallelepiped or a cylinder. See 3.4.3 above.

<sup>14</sup> Let us note that, by definition, the circular path followed by any point being roto-projected is entirely on a same side of the  $xz$  plane. As a consequence, two close points on opposite sides of the  $xz$  plane are roto-projected onto opposite  $xz$  half-planes, i.e. their  $x$  coordinates have opposite signs.

<sup>15</sup> The toleranced feature is the intersection of the surface with a defined plane, see [18] Figures 90 and 92 for examples. The intersection plane can be defined either explicitly by an intersection plane indicator (for example [18] Figures 90) or implicitly by the drawing (for example the generatrix of a cylinder, see [18] Figures 92).

<sup>16</sup> The toleranced feature is a derived line such as the median line of a cylinder (for example, [18] Figures 94).

### 3.4.4 Constrained features

Features may be subject to constraints, e.g., the axis of a cylinder indicated as secondary datum is constrained to be orthogonal to a plane indicated as primary datum<sup>17</sup>.

Apart from the datum system, tolerances of form (without a datum) are free from constraints, orientation tolerances (parallelism, perpendicularity and angularity) are constrained by the datum orientation(s), positions tolerances are constrained by the datum orientation(s) and position(s).

The procedure described in 3.3 is valid for free as well as for constrained features and applies with no distinction to either case. The same is true for the uncertainty evaluation based on the principle of maximum entropy (3.4.1).

### 3.4.5 Profile tolerances

Profile tolerances can be either with or without reference to a datum (system).

When the nominal profile is not merely straight or flat, it contains dimensional information, for instance the diameter of a cylindrical surface, or the concavity of a curved surface. Even when the profile tolerance is without a datum, constraints are there to match the dimensional information.

The uncertainty evaluation for verification of profile tolerances with or without datum is no different from that for form or orientation tolerances. The procedures described in 3.3, and when necessary those in 3.4.1 and/or 3.4.2, apply to the evaluation.

---

<sup>17</sup> The primary datum is in fact the direction normal to the plane, and the cylinder is constrained to be parallel to this direction. The effect of the cylinder as secondary datum is the localisation of the coordinate axis orthogonal to the plane.

## 4. Conclusions

A practical *a posteriori* (type A) method to evaluate the task specific uncertainty of coordinate measurements done with tactile CMMs in ordinary industrial floors was developed. It provides traceable measurement values and their uncertainties with need neither of a calibrated reference workpiece nor of special software. A repetition and reversal plan is carried out with the very workpiece under measurement; the results are computed within a simple spreadsheet.

The developed method is applicable not only to simple dimensional measurements, e.g., size, angle and location, but also to form and profile deviations. The measurement uncertainty is estimated from a combination of the revealed errors and of standard uncertainty components derived from ANOVA analysis.

By resorting to the maximum entropy principle, the method is extended to those cases where the CMM software interface do not disclose internal calculation details such as the local form deviations.

A spreadsheet template implementing the method has been developed. The required operation to get traceable results and their uncertainties is just copying-and-pasting individual measurement results obtained according to the experimental plan.

Even if the method is designed and intended for tactile CMMs, further developments may reveal that its core is applicable to other CMSs as well. A preliminary application to computer tomography was encouraging.

## 5. References

- [1] R. G. Wilhelm, R. J. Hocken and H. Schwenke, "Task Specific Uncertainty in Coordinate Measurement," *CIRP Annals*, vol. 50, no. 2, pp. 553-563, 2001.
- [2] F. Zanini, E. Savio and S. Carmignato, "Uncertainty determination of X-ray computed tomography dimensional measurements of additively manufactured metal lattice structures," in *Proc. of the euspens's 21st International Conference & Exhibition*, Copenhagen, DK, 2021.
- [3] ISO 15530-3:2011, "Geometrical product specifications (GPS) — Coordinate measuring machines (CMM): Technique for determining the uncertainty of measurement — Part 3: Use of calibrated workpieces or measurement standards," 2011.
- [4] ISO 14253-1:2017, "Geometrical product specifications (GPS) — Inspection by measurement of workpieces and measuring equipment — Part 1: Decision rules for verifying conformity or nonconformity with specifications".
- [5] ISO 4287:1997, "Geometrical Product Specifications (GPS) — Surface texture: Profile method — Terms, definitions and surface texture parameters".
- [6] BS 7172:1989, "Guide to assessment of position, size and departure from nominal form of geometric features," 1989.
- [7] ISO 12181-2:2011, "Geometrical product specifications (GPS) — Roundness — Part 2: Specification operators," 2011.
- [8] ISO/DTS 15530-2, "ISO DTS 15530-2:2007, Geometrical Product Specifications (GPS) — Coordinate Measuring Machines (CMM): Technique for Determining the Uncertainty of Measurement — Part 2: Use of Multiple Measurement Strategies.," 2007.
- [9] FP5-GROWTH, *EasyTrac - Easier and cheaper traceability in industry by up to date methods of calibration*, <https://cordis.europa.eu/project/id/G6RD-CT-2000-00188>, 2000-2003.
- [10] O. Sato, T. Takatsuji and A. Balsamo, "Practical experiment design of task specific uncertainty evaluation for coordinate metrology," in *Advanced Mathematical and Computational Tools in Metrology and Testing XII*, vol. 90, 2022, pp. 381-389.
- [11] O. Sato, T. Takatsuji, Y. Miura and S. Nakanishi, "GD&T task specific measurement uncertainty evaluation for manufacturing floor," *Measurement: Sensors*, vol. 18, p. 100141, 2021.
- [12] ISO 14406:2010, "Geometrical product specifications (GPS) — Extraction," 2010.
- [13] ISO 10360-2:2009, "Geometrical product specifications (GPS) — Acceptance and reverification tests for coordinate measuring machines (CMM) — Part 2: CMMs used for measuring linear dimensions," 2009.



- [14] ISO/DIS 10360-11:2021, "Geometrical product specifications (GPS) — Acceptance and reverification tests for coordinate measuring systems (CMS) — Part 11: CMSs using the principle of X-ray computed tomography (CT)," 2021.
- [15] ISO 10360-5:2020, "Geometrical product specifications (GPS) — Acceptance and reverification tests for coordinate measuring systems (CMS) — Part 5: Coordinate measuring machines (CMMs) using single and multiple stylus contacting probing systems using discrete point and/or sc," 2020.
- [16] Y. Ojima, S. Yasui, L. Feng, T. Suzuki and T. Harada, "The Probability of Occurrence of Negative Estimates in the Variance," *Frontiers in Statistical Quality Control*, vol. 8, pp. 322-331, 2006.
- [17] ISO/TR 16015:2003, "Geometrical product specifications (GPS) — Systematic errors and contributions to measurement uncertainty of length measurement due to thermal influences," 2003.
- [18] ISO 1101:2017, "Geometrical product specifications (GPS) — Geometrical tolerancing — Tolerances of form, orientation, location and run-out," 2017.